ChemPhysChem

Research Article
doi.org/10.1002/cphc.202300387

Chemistry Europe
European Chemical Societies Publishing

www.chemphyschem.org

Special Collection

Molecular Oxygen Trimer: Multiplet Structures and Stability

L. Beatriz Castro-Gómez,[a] José Campos-Martínez,[b] Marta I. Hernández,*[b] and Ramón Hernández-Lamoneda*[a]

We present a detailed theoretical study of the molecular oxygen trimer where the potential energy surfaces of the seven multiplet states have been calculated by means of a pair approximation with very accurate dimer ab initio potentials. In order to obtain all the states a matrix representation of the potential using the uncoupled spin representation has been applied. The $S = 0$ and $S = 1$ states are nearly degenerate and low-lying isomers appear for most multiplicities. A crucial point in deciding the relative stabilities is the zero-point energy which represents a sizable fraction of the electronic well-depth. Therefore, we have performed accurate diffusion Monte Carlo studies of the lowest state in each multiplicity. Analysis of the wavefunction allows a deeper interpretation of the cluster structures, finding that they are significantly floppy in most cases.

Introduction

The structure, spectra and dynamics of weakly bound clusters has been a fertile area of theoretical and experimental research.[1] Even though weakly bounded clusters of varying sizes have been studied, most of the detailed characterizations both experimentally and theoretically have been performed on the dimers. Furthermore, most of the detailed studies on neutral trimers have relied on the infrared activity of the monomers.[2,3] In this sense it is worth noticing that most of the studies on neutral molecular oxygen clusters so far have concentrated on the dimer,[4–15] the only exceptions we know about are a theoretical study of large clusters[16] and Stern-Gerlach studies[17,18] where only the total spin of the system is determined. In the more recent study where dimer, trimer and tetramer were analyzed they found a small deflection consistent with singlet states; however, the authors point out that the deflection is larger than the experimental error suggesting non-zero spin states could be present. In the older study the authors conclude that the dimer is paramagnetic in contradiction with the more recent study and many other experimental and theoretical studies.[4,6,8,9,11,13,15]

It is of interest to mention that molecular oxygen tetramer units characterize the high pressure solid epsilon phase.[19,20] This phase has several unique properties such as a magnetic and volumetric collapse with increasing pressure.[21,22] In fact, a simple model based on a tetramer interaction potential plus pairwise interactions[23,24] can accurately reproduce the pressure dependence of the structural parameters as measured experimentally.

The aim of the present work is to take a first step in the detailed theoretical characterization of the molecular oxygen trimer and hopefully this will motivate associated experimental work in the future. The fact that molecular oxygen has a spin equal to one leads to a multiplet structure whose complexity increases with the size of the cluster. Furthermore, the energy differences among the different spin states are small and it is common to observe surface crossings. These characteristics make them particularly interesting for their magnetic and vibronic properties.

In order to study clusters larger than the dimer we rely on a pairwise approximation and highly accurate dimer potentials for the three multiplets ($S = 0, 1, 2$), that we developed in the past.[10–12,25] In fact, this approach has already been applied by us in the case of the trimer for the state of maximum multiplicity[26] where it is clear that the dimer interaction potential to be used is that of the quintet state. In that study we showed that the three body effects for the maximum multiplicity state ($S = 3$) are very small and the pairwise approximation thus very accurate.

Another challenge in the case of weakly bound clusters is the accurate determination of the zero-point energy which represents a sizable fraction of the electronic well depth. Furthermore, the definition of structure becomes blurred due to the presence of quasidegenerate isomers linked by small energetic barriers. For example, in the case of the $S = 3$ state the zero-point energy represented roughly 20% of the electronic well-depth and the ground vibrational wavefunction sampled two different structures of C_2 and D_3 symmetry.[26] Obviously, one has to go beyond the harmonic approximation and use accurate diffusion Monte Carlo methods[27–31] or the more accurate close-coupled equation treatment.[32]

[a] L. B. Castro-Gómez, Dr. R. Hernández-Lamoneda
Centro de Investigaciones Químicas, Universidad Autónoma del Estado de Morelos, 62210 Cuernavaca, Morelos, Mexico
E-mail: ramon@uaem.mx

[b] Dr. J. Campos-Martínez, Dr. M. I. Hernández
Instituto de Física Fundamental, Consejo Superior de Investigaciones Científicas (IFF-CSIC), Serrano 123, 28006 Madrid, Spain
E-mail: marta@iff.csic.es

Supporting information for this article is available on the WWW under https://doi.org/10.1002/cphc.202300387

Special Collection An invited contribution to a Special Collection dedicated to Pablo Villarreal Herrán on the occasion of his 70th birthday

Methodology

Pairwise Additivity Approximation to the Interaction Potential in the Oxygen Trimer

In this work we use the pairwise additivity approximation to calculate the interaction potential energy for all the multiplet states in the oxygen trimer. To do so, we construct the potential matrices of the oxygen dimer in the coupled representation. These matrices are diagonal, and their elements are the interaction potentials obtained previously by our group[12,25] and then, by means of a similarity transformation, change the basis to the uncoupled representation, where block-diagonal matrices are obtained when selecting the uncoupled basis set in a decreasing order of the spin projection operator, S_z.[13]

Once we obtained the interaction potential matrix of the dimer in the uncoupled representation, we use its matrix elements to construct the trimer matrix. We use Eq. 1 to obtain each matrix element V_{ijk} corresponding to the interaction potential in the trimer, which is given by

$$\begin{aligned} V_{123} \quad &= \langle m_{s1}, m_{s2}|V_{12}|m_{s1}', m_{s2}'\rangle\langle m_{s3}|m_{s3}'\rangle \\ &+\langle m_{s1}, m_{s3}|V_{13}|m_{s1}', m_{s3}'\rangle\langle m_{s2}|m_{s2}'\rangle \\ &+\langle m_{s2}, m_{s3}|V_{23}|m_{s2}', m_{s3}'\rangle\langle m_{s1}|m_{s1}'\rangle, \end{aligned} \tag{1}$$

where m_{si} is the projection of spin in the i-th monomer and V_{ij} the interaction potential in the $i-j$ dimer.

There are 27 spin states for the oxygen trimer, and so is the dimension of the interaction potential matrix. However, due to degeneracies in the M_s components only 7 PES have to be considered and we choose those with $M_s = 0$ to shorten the matrix from a 27-dimension to a 7-dimension one, considerably simplifying analysis and calculations.

To assign the energies obtained for the trimer to each of its spin states, we build a S^2 matrix for the trimer in the uncoupled basis. Once the interaction potential and the S^2 matrices are diagonalized, we can relate them via the eigenvectors. This is straightforward for the non-degenerate spin states $S = 0$ and $S = 3$. For the (two) quintet and (three) triplet states, this is accomplished by overlapping each S^2 eigenvector with all the eigenvectors of the potential energy. The overlap amongst states with different spin is always zero. The non-zero overlaps correspond to states of the same spin.

Optimization

Once we can determine the energy of each of the PESs, we obtain stable structures using the conjugate gradient algorithm applied previously to obtain the minima for the septet.[26] The energies obtained are converged within hundredths of meV. Because there are three triplet and two quintet PESs very close to each other in energy, we choose to follow these spin-degenerate states adiabatically due to the unclear definition of the highest overlap of eigenvectors near intersection zones. For this reason, we only report minima in the lowest lying PES for each of the spin-states. In order to characterize the obtained structures, we perform a normal mode analysis to ensure that the structures are true minima in the PES. The normal mode analysis was programmed using a finite difference method and truncated to second order approximation, that is, considering only harmonic effects to obtain zero-point energies (ZPE) for each of the minima.

To help us rationalize the structures found for the trimer, we summarize in Table 1 the geometry and energies for the most important stationary points, in all multiplet states, for the oxygen dimer.[11,12]

The septet will be the easiest state to analyse because in the pairwise approximation only the quintet potential for each of the dimer states participates in the interaction, whilst for the rest of the spin states in the trimer the pairwise potential is a linear combination of the different spin states of the dimer.

Diffusion Monte Carlo (DMC) Calculations

The DMC method is used to obtain the quantum ground states of the different spin multiplicities of the oxygen trimer, thus providing accurate estimations of their ZPE beyond the harmonic approximation previously presented. In this approach, the time-dependent Schrödinger equation is transformed into a diffusion equation by changing the variable time, t, to a imaginary time, $\tau = it$. The diffusion equation is solved by a random walk method where the wavefunction is represented by a set of N replicas (configurations of the particles of the system) which, at each time step $\Delta\tau$, randomly translate according to the kinetic energy term of the Hamiltonian and, in addition, multiply or disappear with a probability depending on the potential energy term.[27] The system ground state is then obtained from the longest lasting term ($\tau \to \infty$) of the propagated wavefunction. More details on the method are given elsewhere.[27,28]

As the oxygen molecules are described as rigid rotors, we have applied the DMC formulation for rigid rotors developed by Buch and coworkers.[29,30] The rotational motion of the replicas is carried out by randomly choosing a vector describing the angle and axis of rotation with a probability related to $\Delta\tau$ and the values of the moments of inertia of the rotor. Another feature of the present application is that different DMC computations are carried out associated to the different spin multiplicities ($S = 0$, 1, 2 and 3). We have proceeded similarly as just described above, specifically, eigenstates of Eq. 1 are computed at each $\Delta\tau$ and for every replica, and the desired potential energy value is determined looking for maximum overlaps with the eigenstates of S^2. As mentioned above, this is straightforward for the nondegenerate singlet and septet states. For the other cases (three $S = 1$ and two $S = 2$ states) we have followed an adiabatic criterion, i.e., the eigenstates of the potential with non-zero overlap with these spin states are identified and the potential energy is assigned to the one having the lowest eigenvalue.

Table 1. Equilibrium geometries for the dimer using Jacobi coordinates. Intermolecular distances in Å and angles in degrees.

		E(meV)	geometry			
			R(Å)	θ_a	θ_b	ϕ
$S=0$	X	−17.3	3.27	90.0	90.0	90.0
	H	−32.3	2.94	90.0	90.0	0.0
$S=1$	X	−17.0	3.27	90.0	90.0	90.0
	H	−22.2	3.14	90.0	90.0	0.0
	X	−16.3	3.29	90.0	90.0	90.0
$S=2$	H	−13.7	3.43	90.0	90.0	0.0
	S	−15.7	3.43	72.0	72.0	0.0

In practice, we have used the code developed by Sandler and Buch,[31] previously employed in calculations of the $(O_2)_3$ septet state[26] as well as in studies of He or H_2 clusters doped with atomic ions.[33–35] For each value of the total spin, we have performed calculations using $N=10^4$ replicas, initially built from a Gaussian distribution centered on the minima structures previously obtained. An initial propagation up to $\tau_{max}=5\times10^5$ a.u. was carried out using a large time step ($\Delta\tau=100$ a.u.) to explore the configuration space and reach an initial stabilization of the energy, which is followed by three successive propagations using ever shorter time steps. The ground state energy was estimated by averaging over half of the propagation using the shortest time step ($\Delta\tau=12.5$ a.u.). For each spin, six independent runs were carried out from which an average energy and a standard deviation was obtained. It has been checked that these energies are well converged with respect to the number of replicas, time step and number of runs. Moreover, we have run test calculations starting with a distribution of replicas centered around different minima of a given spin state (e.g., the three minima of $S=1$ in Table 4) and have checked that all simulations converge to the same energy, i.e., the ground state energy. Finally, probability distributions over the configurational space were obtained by means of the descendant weighting algorithm,[28] using eight generations for each DMC run, from which a reasonable estimation of the squared wavefunction is obtained.[30]

Results and Discussion

Stable Structures for the $(O_2)_3$ Cluster

We now present all the minima found for each of the different spin states.

Table 2. Equilibrium structures found for the $(O_2)_3$ septet.

	Symmetry	E(meV)	pairwise contributions			
			R(Å)	θ_a	θ_b	ϕ
I	C_2	−46.83	3.43	72.2	72.2	18.2
			3.42	73.5	73.5	19.3
			3.42	106.5	106.5	19.3
II	D_3	−46.22	3.39	102.8	77.1	133.5
			3.39	77.1	77.1	46.5
			3.39	77.2	102.8	133.4
III	C_{2v}	−42.65	3.30	90.0	92.4	90.0
			3.30	90.0	92.4	90.0
			4.18	36.8	143.2	0.0

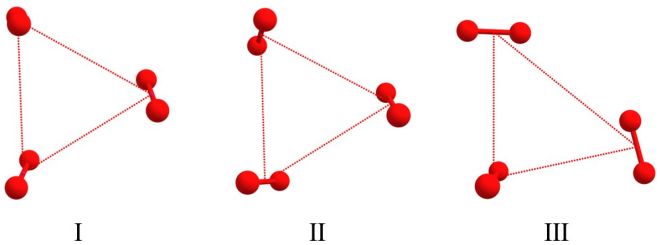

Figure 1. Stable structures for the septet state of the $(O_2)_3$.

Table 2 shows the properties of the stable structures of the septet, represented in Figure 1. Minimum I is a contribution of three S-geometry quintet pair interactions, with very small deviations from the S stationary point in the dimer for the $S=2$ state. Minimum II is very similar in energy to minimum I, but with higher symmetry. Minimum III is a structure which tries as far as possible to arrange the pairs of monomers in an X configuration, which is the global minimum for the dimer in its highest multiplicity state. We reproduce exactly the results obtained previously by our group,[26] confirming the validity of our new method.

For the quintet state we found two minima, illustrated in Figure 2 and described in Table 3. Structure I of the quintet is of lower energy than all the minima found for the state of maximum spin multiplicity. This can be explained by the geometry of the pairs in the cluster. One interaction is given in H geometry, the one preferred by states $S=0,1$ in the dimer, with R almost the value of the minimum for the triplet interaction. Besides, it is more stable than the minimum in X for the $S=2$ state of the dimer. This pairs gives the trimer a C_s geometry. We can observe that structure II is very similar in shape and energy to structure III of the septet, the former being slightly more stable.

We found three minima in the lowest lying PES for the triplets. These are characterized in Table 4 and depicted in Figure 3. Structures I and II are very similar in energy, but present different geometry. Still, the pairwise interactions are almost given in H geometry in addition to a small torsional angle in the case of minimum I, which allows the monomers to be closer to each other. Minimum II stands out for its very symmetric pairwise contributions. All are given in H geometry and only the value of R changes for one of the pairs, giving this structure a C_{2v} symmetry. For the first two pairs R is 3.30 Å, a value between the ones for the triplet and quintet minima in

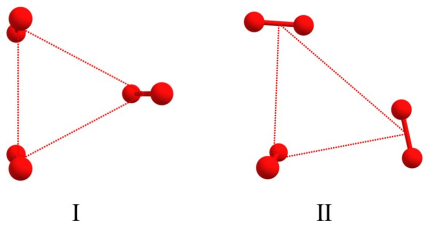

Figure 2. Stable structures for the quintet state of the $(O_2)_3$.

Table 3. Equilibrium structures found for the $(O_2)_3$ quintet.

	Symmetry	E(meV)	pairwise contributions			
			R(Å)	θ_a	θ_b	ϕ
I	C_s	−54.07	3.13	90.0	90.0	0.0
			3.41	105.1	105.1	0.0
			3.41	105.1	105.1	0.0
II	C_{2v}	−44.34	3.30	90.0	91.8	90.0
			3.30	90.0	91.8	90.0
			4.11	36.8	143.2	0.0

Table 4. Equilibrium structures found for the $(O_2)_3$ triplet.

	Symmetry	E(meV)	pairwise contributions			
			R(Å)	θ_a	θ_b	ϕ
			3.05	88.7	89.6	6.9
I	C_2	−66.92	3.05	91.3	90.4	7.0
			3.42	97.6	97.6	9.4
			3.30	90.0	90.0	0.0
II	C_{2v}	−66.52	3.30	90.0	90.0	0.0
			2.92	90.0	90.0	0.0
			3.30	90.0	91.2	90.0
III	C_{2v}	−45.51	3.30	90.0	91.2	90.0
			4.08	37.0	143.0	0.0

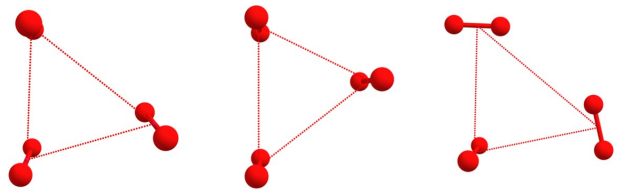

Figure 3. Stable structures for the triplet state of the $(O_2)_3$.

the dimer, amongst which the triplet is the most stable one, and the other is 2.92 Å, the minimum for the singlet. This seems to indicate that this structure is conformed mainly by contributions of the triplet and singlet states in the dimer.

Once more, we found a structure, minimum III, very similar to minimum III in the septet and II in the quintet. It is notorious that even though the energy in this geometry decreases with the spin, it is still very similar in all the states, with differences of less than 1 meV. Also, this is the highest energy structure found for each of the spin states.

Only one minimum corresponding to the singlet state was found. Table 5 and Figure 4 show this result. The structure is highly symmetric, belonging to the D_{3h} point group and is the most stable structure, considering only the electronic energy, amongst all spin states with a potential interaction energy of −67.15 meV.

All the pairwise interactions correspond to equivalent H configurations in the dimer, with $R = 3.13$ Å. This distance is almost exactly the one for the minimum of the triplet state in the dimer. Recalling that the H configuration is a minimum for the oxygen dimer in the singlet and triplet spin states, the minimum found for the trimer is expected in the sense that it mimics the local structure in all the pair contributions that is a minimum for low spin states, increasing the stability of the cluster.

Zero-Point Energies

In addition to the calculated potential well energies, we considered the contribution of the zero-point energy to the potential interaction in the harmonic approximation. The results are shown in Table 6. It is evident that the ZPE accounts for a significant percentage of the interaction potential well. An important consequence is that the stability order among the minima found for the different spin states is inverted in the case of states I and II of the triplet and the singlet. Also, the differences in energy between the minima both among same and different spin states decreases compared to the ones considering only the energy of the well. This is a remarkable result, highlighting the importance of ZPE effects in van der Waals complexes. It is well-known that anharmonic effects are large in weakly bounded systems, furthermore, they can be floppy. For this reason, we decided to perform highly accurate DMC calculations of the ZPE.

Table 5. Equilibrium structure found for the $(O_2)_3$ singlet.

	Symmetry	E(meV)	pairwise contributions			
			R(Å)	θ_a	θ_b	ϕ
			3.13	90.0	90.0	0.0
I	D_{3h}	−67.15	3.13	90.0	90.0	0.0
			3.13	90.0	90.0	0.0

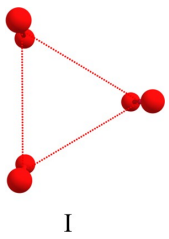

Figure 4. Stable structure for the singlet state of the $(O_2)_3$.

Table 6. Potential well energies (E), zero-point energies (ZPE) and corrected energies for the minima in the $(O_2)_3$ cluster within the harmonic approximation (E_c). DMC energies of the different spin states of $(O_2)_3$ obtained as the average of a set of six independent calculations (E_{DMC}). The standard deviation of the set is given in brackets and refer to the last decimal place.

Spin	Structure	E(meV)	ZPE(meV)	E_c(meV)	E_{DMC} (meV)
	I	−46.83	17.53	−29.30	−32.05(1)
3	II	−46.22	16.66	−29.56	
	III	−42.65	13.76	−28.89	
2	I	−54.07	21.55	−32.52	−36.57(3)
	II	−44.34	14.73	−29.61	
	I	−66.92	28.46	−38.46	−42.40(3)
1	II	−66.52	27.45	−39.07	
	III	−45.51	15.00	−30.51	
0	I	−67.15	30.44	−36.71	−40.15(2)

DMC Bound States

DMC ground state energies of the different spin states of $(O_2)_3$ are gathered in Table 6. By comparison of these energies with the ones obtained within the harmonic approximation (the lowest harmonic energies for each S in Table 6), it can be seen that anharmonicity causes a significant lowering of the ground energy levels (in absolute value, harmonic binding energies are about 10% smaller than the DMC ones). On the other hand, the sequence of ground states for the various multiplicities does agree with the estimations based in the harmonic approximations, i.e., the lowest energy of the complex corresponds to the triplet state, followed by the singlet, quintet and septet states. Note that the lowest energy, based on the minima of the PESs, corresponds to the singlet state (−67.15 meV) closely followed by that of the triplet state (−66.92 meV). The inversion of this order in the quantum calculations must be due to a looser shape of the triplet PES around the minima, accordingly to its smaller ZPE as compared with the singlet one.

More insight into the ground states of the different multiplicities is gained from pictures of their probability distributions, shown in Figure 5.

The bottom panels (d1, d2, d3) correspond to the singlet state distributions as functions of the three intermolecular distances R_{ij} (d1), the angles formed between the intramolecular axes with the vector perpendicular to the triangle formed by the O_2 centers of mass (CM), ϕ_i (d2), and with each median of that triangle, β_i (d3). It is seen that the distribution is peaked around $\phi_i = 0$, i.e. all O_2 axes are perpendicular to the complex plane and that, consistently, the most probable values of β_i are close to $\pi/2$. For comparison with the equilibrium structures of the cluster, Table 7 shows the values of these angles for all the minima and multiplicities.

The angular distributions, together with the fact that the three radial distributions are identical, leads us to conclude that the singlet state resembles quite well the equilibrium geometry of the complex (Table 5). Note, however, the role of anharmonicity that shifts the maximum of the radial distributions to ≈3.4 Å, larger than 3.13 Å, the value expected within the harmonic approximation.

Analysis of the probability distributions of the other multiplicities is more complex, mainly due to the existence of various equivalent minima in the corresponding PESs resulting from permutations of the molecules. For example, the structure I of the triplet PES (Table 4), with intermolecular distances $R_{12} = R_{13} = 3.05$ and $R_{23} = 3.42$ Å, leads, after a 1↔2 exchange, to a different point of the PES with $R_{12} = R_{23} = 3.05$ and $R_{13} = 3.42$ Å. For these situations it is very convenient the use of hyperspherical coordinates which treat in an equivalent manner all channels/minima due to particle exchange.[36,37] In the present study we describe the position of the CMs of the molecules by means of the hyperradius and two hyperangles[37]

$$\rho = \left(\widehat{Q}^2 + \widehat{q}^2\right)^{1/2},$$
$$\tan\Theta = \frac{\left[\left(\widehat{Q}^2 + \widehat{q}^2\right)^2 + \left(2\widehat{\mathbf{Q}}^2 \cdot \widehat{\mathbf{q}}^2\right)^2\right]^{1/2}}{2\widehat{Q}\widehat{q}\sin\theta}, \quad (2)$$
$$\tan(2\chi) = \frac{2\widehat{\mathbf{Q}}^2 \cdot \widehat{\mathbf{q}}^2}{\widehat{Q}^2 - \widehat{q}^2},$$

where $\hat{\mathbf{Q}}$ and $\hat{\mathbf{q}}$ are mass-scaled Jacobi coordinates, $\hat{\mathbf{Q}} = d\mathbf{Q}$ and $\hat{\mathbf{q}} = \mathbf{q}/d$, $d = 2/\sqrt{3}$ being the scaling factor and $\mathbf{Q}$ and $\mathbf{q}$, the Jacobi coordinates for a chosen arrangement (for instance, $\mathbf{q}$ is the vector joining molecules 1 and 2, and $\mathbf{Q}$, the vector joining molecule 3 with the CM of molecules 1 and 2). The hyperradius ρ and the hyperangles Θ and χ describe the size and shape of the triangle formed by the three molecules, respectively. In particular, χ enables to distinguish the regions of the PES that are related by particle exchange.

An illustration of the dependence of triplet PES with the hyperangles is presented in the right panel of Figure 6. For every value of (Θ, χ), the potential energy has been minimized with respect to ρ (the intramolecular axes were kept perpendicularly to the cluster plane to ease the computations). It can be seen that, along most of the Figure, the PES takes quite low

Table 7. Equilibrium values of the internal angles ϕ_i and β_i for each of the i-th O_2 monomers in the trimer's minima. ϕ represents the angle formed between the intramolecular vector of each of the molecules with the vector perpendicular to the plane containing the three centers of mass of the molecules (CM). β is defined as the angle between the intramolecular axes and the vector pointing from the center of mass of the cluster to the center of mass of the monomer (median).

Spin	Structure	ϕ_1	ϕ_2	ϕ_3	β_1	β_2	β_3
3	I	19.9	19.9	34.5	109.9	70.1	90.0
	II	26.4	153.5	26.3	90.1	90.1	90.0
	III	180.0	90.0	90.0	90.0	121.0	121.0
2	I	17.1	17.1	17.1	80.9	80.9	107.1
	II	0.0	90.0	90.0	90.0	120.5	120.5
1	I	2.4	8.9	8.9	90.0	85.3	94.7
	II	0.0	0.0	0.0	90.0	90.0	90.0
	III	0.0	90.0	90.0	90.0	120.0	120.0
0	I	0.0	0.0	0.0	90.0	90.0	90.0

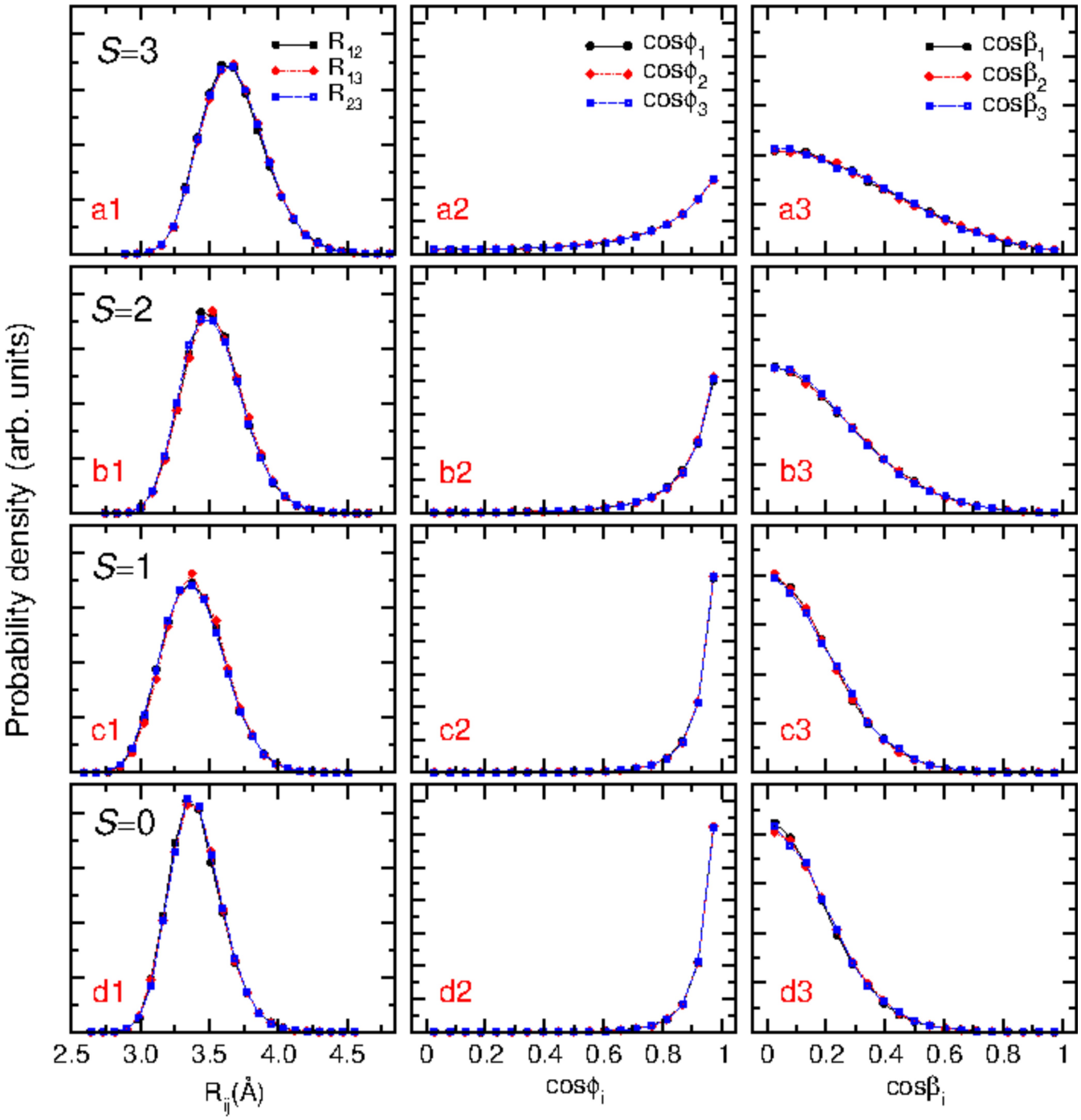

Figure 5. Histograms of the probability distributions of the ground states of the septet (a1, a2, a3), quintet (b1, b2, b3), triplet (c1, c2, c3) and singlet (d1, d2, d3) states of the oxygen trimer, as obtained from the DMC calculations. Left column (a1, b1, c1, d1): Probability densities as functions of the distances between every pair of molecules [$(i; j) = (1,2)$, (1,3) and (2,3)]. Central column (a2, b2, c2, d2): Probability distributions as functions of the cosine of the angle formed between the intramolecular axis of each molecule ($i = 1$, 2, and 3) and the axis perpendicular to the plane formed by the CMs of the molecules. Right column (a3, b3, c3, d3): Probability densities as functions of the cosine of the angles formed between the molecules axes ($i = 1$, 2, and 3) and the vector pointing from the CM of the complex to the CM of each molecule (median of the triangle formed by the molecules). See text for discussion.

values of the energy (below −50 meV) and that around $(\Theta/\pi) \approx 0.05$, it is very shallow for all values of χ. As expected from these features, it is found that the ground state DMC wavefunction covers all the range of χ and most of values of Θ shown in the Figure, in other words, that the triplet ground state is extremely floppy.

Interestingly, if the wavefunction is examined for restricted ranges of χ, its distributions can be connected with the local minima found in the study of the PES (Table 4). For example, the radial distributions within the range $-3/12 \leq \chi/\pi \leq -1/12$ are depicted in the lower-left panel of Figure 6. There are two identical distributions (R_{12} and R_{13}) peaked around 3.3 Å and

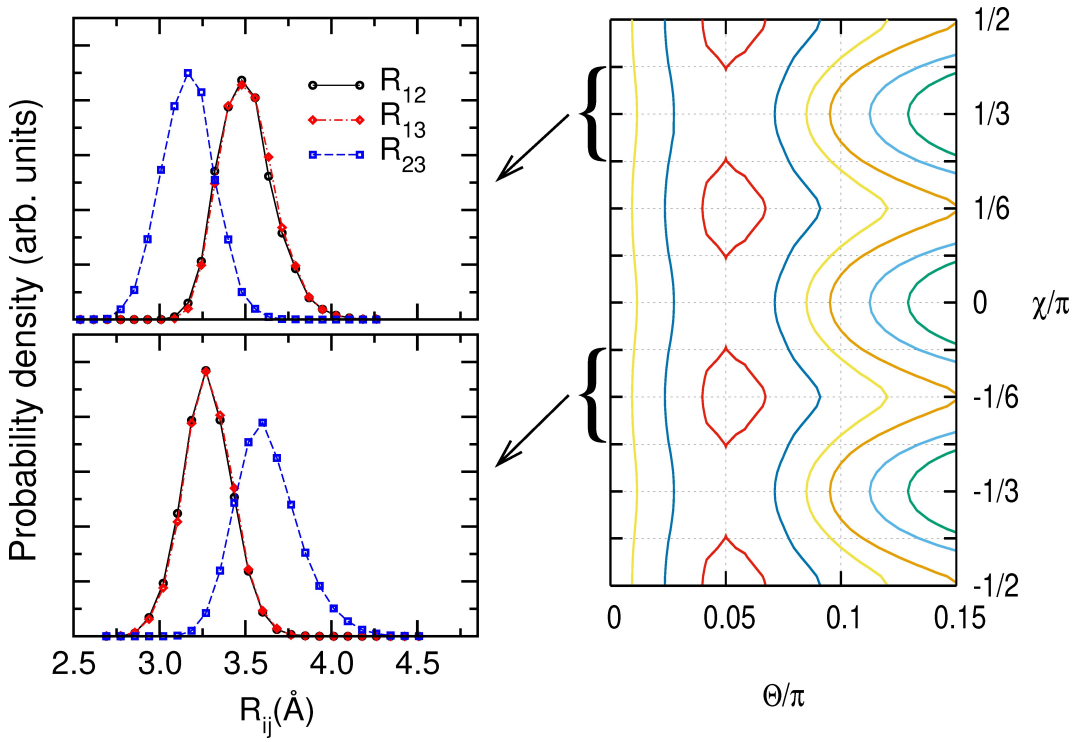

Figure 6. Right panel: $S = 1$ PES as a function of the hyperangles Θ and χ (Eq. 2); contours are at -66.5 (red), -65 (dark blue), -62.5 (yellow), -60 (orange), -55 (light blue) and -50 meV (green). Left panel: histograms of the probability densities vs. intermolecular distances for the part of the triplet DMC ground state fulfilling that $\chi/\pi \in [3/12, 5/12)$ (top) or $\chi/\pi \in [-3/12, -1/12)$(bottom). See text for details and discussion.

another one (R_{23}) around 3.6 Å; this is so because they sit around the minimum structure I of the PES. Anagolously, when resticting to the range $3/12 \leq \chi/\pi \leq 5/12$, the R_{12} and R_{13} distributions (upper-left panel of Figure 6) have their maxima around 3.5 Å, and the R_{23} one, around 3.2 Å, showing that the wavefunction also spans the minimum structure II of the PES. Radial distributions along other regions of the χ hyperangle are like the ones depicted for the different labelings corresponding to the permutation of the molecules. In summary, the triplet wavefunction spans both I and II structures as well as their equivalent minima, without signature of barriers between the different basins. As a consequence, the radial distributions of the complete wavefunction (c1 of Figure 5) are identical for all the intermolecular distances and wider than those of the singlet state. The distributions for the angles ϕ_i and β_i (c2 and c3 of Figure 5) do resemble the ones of the singlet state.

An analogous analysis, based on hyperspherical coordinates, has been carried out for the quintet and septet wavefunctions. First, it is found that the quintet state evenly extends over all the equivalent minima of structure I of Table 3, including the regions between them. The resulting distribution of distances is quite similar to the triplet one, shifted to somewhat larger distances (b1 of Figure 5). The angular distributions (b2 and b3 of Figure 5) are similar but a bit more delocalized than the singlet and triplet ones. No signature of probability density has been observed around the geometry corresponding to structure II: indeed, no probability is found for the molecular axes being paralell to the cluster plane ($\phi_i \approx \pi/2$) as should be if the state extended across structure II. Finally, it is found that the septet wavefunction extends over both structures I and II of Table 2 and their equivalent minima. The angular distributions (a2 and a3 of Figure 5) are wider than the ones of other multiplicities and a small but non negligible probability for ϕ_i close to $\pi/2$, suggest that the wavefunction may, in a minor extent, span geometries close to structure III.

Summary and Conclusions

We have applied a general method based on the uncoupled spin representation to calculate the multiplet structure of the molecular oxygen trimer using a pairwise approximation and highly accurate pair potentials. At the purely electronic level the ground state of the system is predicted to be a singlet with D_{3h} symmetry; however, there are two triplets which are nearly degenerate, within only a few tenths of meV. The rest of states follow a monotonous increase in energy with the total spin. This is analogous to the case of the dimer and can be related with the dominance of antiferromagnetic couplings. Addition of ZPE using the harmonic approximation interchanges the $S = 0$ and the $S = 1$ states, so that now the ground state is predicted to be a triplet. Again, the quasidegeneracy with the $S = 0$ state remains but the energy difference is now of the order of a couple of meV.

An accurate treatment of the vibrational motion using DMC confirms that the energy ordering for the $S = 0$ and $S = 1$ states changes when including zero-point energies but the states remain quasi-degenerate. In this sense it is worth mentioning

that the previous Stern-Gerlach study[18] was consistent with the presence of both types of states although it favored the singlet state. An accurate treatment of this difficult problem should include three-body corrections to the potentials and a new determination of the associated zero-point energies. A detailed analysis of the DMC wavefunctions indicates that for the non-zero spin states in the ground vibrational state all the permutationally equivalent minima are explored; however, it is still possible to assign which structures or isomers are sampled and which are not.

Acknowledgements

This work was supported by the Spanish MICINN with Grant PID2020-114957GB–I00/AEI/10.13039/501100011033, (JCM, MIH). Allocation of computing time by CESGA (Spain) is also acknowledged. (LBCG) was supported by CONAHCYT, (Mexico, Ref. 1080446).

Conflict of Interests

The authors declare no conflict of interest.

Data Availability Statement

The data that support the findings of this study are available in the supplementary material of this article.

Keywords: van der Waals clusters · Diffusion Monte Carlo · Spin coupling · *ab initio* potentials · multiplet states

[1] *Chem. Rev.* **2000**, *100*, (Complete Issue) 7.
[2] N. Pugliano, R. J. Saykally, *Science* **1992**, *257*, 1937.
[3] N. Moazzen-Ahmadi, A. R. W. McKellar, *Int. Rev. Phys. Chem.* **2013**, *32*, 611.
[4] C. A. Long, G. E. Ewing, *J. Chem. Phys.* **1973**, *58*, 4824.
[5] A. Campargue, L. Biennier, A. Kachanov, R. Jost, B. Bussery-Honvault, V. Veyret, S. Churassy, R. Bacis, *Chem. Phys. Lett.* **1998**, *228*, 734.
[6] L. Biennier, D. Romanini, A. Kachanov, A. Campargue, B. Bussery-Honvault, R. Bacis, *J. Chem. Phys.* **2000**, *112*, 6309.
[7] V. Aquilanti, D. Ascenzi, M. Bartolomei, D. Cappelletti, S. Cavalli, M. de Castro Vitores, F. Pirani, *Phys. Rev. Lett.* **1999**, *82*, 69.
[8] V. Aquilanti, D. Ascenzi, M. Bartolomei, D. Cappelletti, S. Cavalli, M. de Castro Vitores, F. Pirani, *J. Am. Chem. Soc.* **1999**, *121*, 10794.
[9] P. Wormer, A. van der Avoird, *J. Chem. Phys.* **1984**, *81*, 1929.
[10] R. Hernández-Lamoneda, M. Bartolomei, M. I. Hernández, J. Campos-Martínez, F. Dayou, *J. Phys. Chem. A* **2005**, *109*, 11587.
[11] M. Bartolomei, M. Hernández, J. Campos-Martínez, E. Carmona-Novillo, R. Hernández-Lamoneda, *Phys. Chem. Chem. Phys.* **2008**, *10*, 5374.
[12] M. Bartolomei, E. Carmona-Novillo, M. I. Hernández, J. Campos-Martínez, R. Hernández-Lamoneda, *J. Chem. Phys.* **2010**, *133*, 124311.
[13] M. A. Valentín-Rodríguez, M. Bartolomei, M. I. Hernández, J. Campos-Martínez, R. Hernández-Lamoneda, *J. Chem. Phys.* **2020**, *152*, 184304.
[14] B. Bussery, P. Wormer, *J. Chem. Phys.* **1993**, *99*, 1230.
[15] J. Goodman, L. E. Brus, *J. Chem. Phys.* **1977**, *67*, 4398.
[16] F. Calvo, G. Torchet, *J. Cryst. Growth* **2007**, *299*, 374.
[17] A. V. Deursen, J. Reuss, *Int. J. Mass Spectrom. Ion Processes* **1977**, *23*, 109.
[18] A. Malakhovskii, E. Sominska, A. Gedanken, *J. Chem. Soc. Faraday Trans.* **1996**, *92*, 1319.
[19] L. F. Lundegaard, G. Weck, M. I. McMahon, S. Desgreniers, P. Loubeyre, *Nature* **2006**, *443*, 201.
[20] H. Fujihisa, Y. Akahama, H. Kawamura, Y. Ohishi, O. Shimomura, H. Yamawaki, M. Sakashita, Y. Gotoh, S. Takeya, K. Honda, *Phys. Rev. Lett.* **2006**, *97*, 085503.
[21] Y. Crespo, M. Fabrizio, S. Scandolo, E. Tosatti, *Proc. Natl. Acad. Sci. USA* **2014**, *111*, 10427.
[22] I. N. Goncharenko, *Phys. Rev. Lett.* **2005**, *94*, 205701.
[23] M. Bartolomei, E. Carmona-Novillo, M. I. Hernández, J. Pérez-Ríos, J. Campos-Martínez, R. Hernández-Lamoneda, *Phys. Rev. B* **2011**, *84*, 092105.
[24] M. A. Valentín-Rodríguez, M. Bartolomei, M. I. Hernández, J. Campos-Martínez, R. Hernández-Lamoneda, *J. Chem. Phys.* **2021**, *154*, 104307.
[25] M. Bartolomei, E. Carmona-Novillo, M. I. Hernández, J. Campos-Martínez, R. Hernández-Lamoneda, *J. Chem. Phys.* **2008**, *128*, 124304.
[26] R. Hernández-Lamoneda, J. Pérez-Ríos, E. Carmona-Novillo, M. Bartolomei, J. Campos-Martínez, M. I. Hernández, *Chem. Phys.* **2012**, *399*, 80.
[27] J. B. Anderson, *J. Chem. Phys.* **1975**, *63*, 1499.
[28] M. A. Suhm, R. O. Watts, *Phys. Rep.* **1991**, *204*, 293.
[29] V. Buch, *J. Chem. Phys.* **1992**, *97*, 726.
[30] P. Sandler, V. Buch, J. Sadlej, *J. Chem. Phys.* **1996**, *105*, 10387.
[31] P. Sandler, V. Buch, *General purpose QCLUSTER pro- gram for Rigid Body Diffusion Monte Carlo simulation of an arbitrary molecular cluster*, private communication **1999**.
[32] E. Carmona-Novillo, M. Bartolomei, M. I. Hernández, J. Campos-Martínez, R. Hernández-Lamoneda, *J. Chem. Phys.* **2012**, *137*, 114304.
[33] S. J. Kolmann, J. H. D'Arcy, M. J. T. Jordan, *J. Chem. Phys.* **2013**, *139*.
[34] J. Ortiz de Zárate, M. Bartolomei, T. González-Lezana, J. Campos-Martínez, M. I. Hernández, R. Pérez de Tudela, J. Hernández-Rojas, J. Bretón, F. Pirani, L. Kranabetter, P. Martini, M. Kuhn, F. Laimer, P. Scheier, *Phys. Chem. Chem. Phys.* **2019**, *21*, 15662.
[35] M. Bartolomei, P. Martini, R. Pérez de Tudela, T. González-Lezana, M. I. Hernández, J. Campos-Martínez, J. Hernández-Rojas, J. Bretón, P. Scheier, *Molecules* **2021**, *26*.
[36] R. C. Whitten, F. T. Smith, *J. Math. Phys.* **1968**, *9*, 1103.
[37] R. T. Pack, G. A. Parker, *J. Chem. Phys.* **1987**, *87*, 3888.

Manuscript received: June 2, 2023
Revised manuscript received: September 1, 2023
Accepted manuscript online: September 7, 2023
Version of record online: ■■, ■■

RESEARCH ARTICLE

The dependence of the triplet PES with the hyperangles is used to interpret the ground state DMC wave-function, revealing it to be very floppy. When restricted ranges are analysed, the distributions connect with the local minima of C_{2v} and C_2 symmetries. On the contrary, the vibrationally averaged structures are consistent with an equilateral triangle due to permutational symmetry.

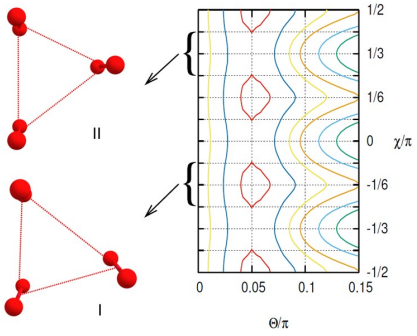

L. B. Castro-Gómez, Dr. J. Campos-Martínez, Dr. M. I. Hernández, Dr. R. Hernández-Lamoneda**